Articles in PresS. J Neurophysiol (May 15, 2013). doi:10.1152/jn.00520.2012

Individual differences in attention strategies during detection, fine discrimination, and coarse discrimination

David A. Bridwell[1,2], Elizabeth A. Hecker[1], John T. Serences[3,4], and Ramesh Srinivasan[1]

[1]Department of Cognitive Sciences, University of California, Irvine
[2]The Mind Research Network, Albuquerque, New Mexico
[3]Department of Psychology, University of California, San Diego
[4] Neuroscience Graduate Program, University of California, San Diego

Please address correspondence to David Bridwell, The Mind Research Network, 1101 Yale Blvd. NE, Albuquerque, New Mexico 87106. E-mail: dbridwell@mrn.org.

Running Head: Attentional strategies

Abstract

Interacting with the environment requires the ability to flexibly direct attention to relevant features. We examined the degree in which individuals attend to visual features within and across Detection, Fine Discrimination, and Coarse Discrimination tasks. Electroencephalographic (EEG) responses were measured to an unattended peripheral flickering (4 or 6 Hz) grating while individuals (n=33) attended to orientations that were offset by 0, 10, 20, 30, 40 and 90 degrees from the orientation of the unattended flicker. These unattended responses may be sensitive to attentional gain at the attended spatial location, since attention to features enhances early visual responses throughout the visual field. We found no significant differences in tuning curves across the three tasks in part due to individual differences in strategies. We sought to characterize individual attention strategies using hierarchical Bayesian modeling, which grouped individuals into families of curves that reflect attention to the physical target orientation ("on-channel"), away from the target orientation ("off-channel"), or a uniform distribution of attention. The different curves were related to behavioral performance; individuals with "on-channel" curves have lower thresholds than individuals with uniform curves. Individuals with "off-channel" curves during Fine Discrimination additionally have lower thresholds than those assigned to uniform curves, highlighting the perceptual benefits of attending away from the physical target orientation during fine discriminations. Finally, we show that a subset of individuals with optimal curves ("on-channel") during Detection also demonstrate optimal curves ("off-channel") during Fine Discrimination, indicating that a subset of individuals can modulate tuning optimally for detection and discrimination.

Keywords:

Attentional gain, Attentional flexibility, Perception, EEG, SSVEP

Introduction

Attention biases early visual processing so that relevant information is enhanced and irrelevant information is suppressed or ignored. The neural representations of these attentional biases are routinely demonstrated in early visual areas (e.g. V1) due to their high selectivity to basic visual features (such as orientation). For example, detecting a target of known orientation results in an increased response in neurons selective to the target orientation and a reduced response in neurons sensitive to orientations away from the target (Cohen & Maunsell, 2011; Haenny & Schiller, 1988; Martinez-Trujillo & Treue, 2004; Maunsell, Sclar, Nealey, & DePriest, 1991; Motter, 1993, 1994). Thus, attention often enhances the neural representation of the physical features of visual targets. A growing body of evidence demonstrates that attention may also enhance the representation of features away (or "off-channel") from the physical features of potential targets, in cases where those neurons provide the most relevant information. For example, when discriminating between two gratings nearby in orientation (fine discrimination) it is theoretically more advantageous to enhance the representation of orientations *away* from the physical orientations of the two gratings, since they demonstrate the largest difference in response (i.e. firing rate) between the two potential targets (Jazayeri & Movshon, 2006; Regan & Beverley, 1985).

Psychophysical results are consistent with the theoretical account that "off-channel" orientations are most informative for fine discriminations of orientation (Regan & Beverley, 1985), directions of motion (Hol & Treue, 2001), and spatial frequency (Wilson & Regan, 1984). The neural benefits of "off-channel" responses has been demonstrated by the ability of "off-channel" single unit activity to predict motion direction discrimination (Purushothaman & Bradley, 2005), and improved orientation coding in "off-channel" neurons during the perceptual learning of fine discriminations (Raiguel, Vogels, Mysore, & Orban, 2006; Schoups, Vogels, Qian, & Orban, 2001). The psychophysical benefits may be related to enhanced "off-channel" responses with attention as demonstrated in BOLD fMRI V1 tuning profiles when individuals were cued to the direction of the nearby change in orientation (Scolari, Byers, & Serences, 2012), and as suggested by an increased response to gratings oriented 20 deg. away from fine discrimination orientations (Verghese, Kim, & Wade, 2012). These findings suggest that attention shapes early visual processing in a relatively flexible manner, which helps ensure that individuals can deal with the complex discriminations and detections that can usefully be applied to a visual scene.

The following study used the frequency tagging technique to isolate the response of large-scale brain networks to a grating outside the spatial focus of attention while attention is parametrically varied over orientations. The flicker contains a *fixed orientation*, thus, the flickering input in principle originates from early visual neurons sensitive to the flicker *features* and propagates within the large scale brain networks sensitive to the flicker *frequency* (Nunez & Srinivasan, 2006; Srinivasan, Bibi, & Nunez, 2006). Attending to a particular orientation at the center of the screen enhances the neural response to that orientation throughout the visual field, including neurons that respond to the spatial location of the unattended flicker (Bichot, 2005; Martinez-Trujillo & Treue, 2004; Saenz, Buracas, & Boynton, 2002; Serences & Boynton, 2007; Treue & Martinez-Trujillo, 1999). This widespread influence of attention to one feature has also been demonstrated in steady-state visual evoked potential (SSVEP) responses to a flicker presented at an unattended location (Bridwell & Srinivasan, 2012). In this study, the SSVEP response to an unattended flickering grating may provide a measure of the attentional tuning profile, or "attentional tuning curve" over orientations. We measured these tuning profiles while individuals performed Detection (D), Coarse Discriminations (CD), and Fine Discriminations (FD), which theoretically differ in the degree of complexity of the attentional tuning (e.g. applying a single peak during Detection, or two peaks during the Discrimination tasks), or the orientation where gain should optimally be applied (e.g. "on-channel" for Detection and Coarse Discrimination, but "off-channel" during Fine Discrimination) (Fig. 1 and 2).

Comparing the shape of the SSVEP estimate of attention tuning curves for Detection, Fine

Discrimination, and Coarse Discrimination allowed us to estimate the strategies that individuals employ during different tasks, to determine whether those strategies are related to individual differences in behavioral performance, and to examine whether individuals can flexibly distribute attention in an optimal manner across the different tasks.

Methods

Participants. 34 individuals (14 females, 1 left handed) between the ages 18 - 35 (mean age: 24, median age: 22) were recruited to participate in four sessions, comprised of one psychophysical (threshold) and three SSVEP sessions. Two individual sessions were excluded due to experimental error, reducing the number of participants to 33 for Detection and Fine Discrimination. Each individual reported normal or corrected to normal vision and had no family history of epilepsy. Informed written consent was obtained at the start of the first session. The individuals ability to maintain fixation was monitored within each session with an SMI eye-tracker (iView Red) camera. Each individual participated in one of four conditions; a left visual field f_l = 4 Hz (contrast reversal; square wave) flicker with a 0 deg unattended grating (n = 19) or a 45 deg unattended grating (n = 4), or a left visual field f_l = 6 Hz flicker with a 0 deg unattended grating (n = 7), or a 45 deg unattended grating (n = 4).

Stimuli. Stimuli were produced by a Power Mac G4 using MATLAB (version; 5.2.1.1421; The MathWorks, Natick, MA) and Psychophysics Toolbox (Brainard, 1997; Pelli, 1997), and displayed on a 19 in. monitor (Viewsonic PF790) with a vertical refresh of 60 Hz. Subjects viewed the monitor from a distance of 57 cm.

Three black concentric circles were displayed centered on fixation (Fig 1). The inner circle (radius = 3.5dva) enclosed the location where Gabor targets would appear and the two outer circles (radius = 5.3 and 12.5dva) enclosed the location of the unattended flickering half annulus. A static checkerboard was displayed within the center circle. The checkerboard was introduced after initial pilot studies showed that individuals had a more difficult time detecting targets when they appear within a high contrast texture. Thus, the checkerboard helped increase task difficulty and helped ensure that individuals detection thresholds are above the lowest contrast value that can be presented. The checkerboard was 80% of the maximum achievable contrast. The minimum and maximum luminance were .3 and 83 cd/m^2, respectively, with a gray background of 39 cd/m^2. The individual squares that comprise the checkerboard were 1.4 dva (40 X 40 pixels).

An unattended flickering grating (f_1 = 4 Hz or f_1 = 6 Hz) was presented in the left visual field during each trial. The spatial frequency of the grating was .35 cycles per degree, which matched the center frequency of the Gabor targets that appeared within the inner circle, centered on fixation. The Gabor targets contained a falloff away from center specified by a Gaussian with a standard deviation of 1.7 dva. The Gabor target was displayed averaged against the background texture, and the background texture was averaged against the gray background when the Gabor was not present.

Task. Individuals performed either a Detection, or a Coarse or Fine Discrimination task. During Detection individuals detected a single Gabor target presented within the static background checkerboard. During Coarse Discrimination individuals discriminated between two potential Gabor targets that were oriented either 45 degrees clockwise (cw) or counterclockwise (ccw) from a reference orientation. During Fine Discrimination individuals discriminated between two potential Gabor targets that were oriented either 4 degrees cw or ccw from a reference orientation (see Fig. 1). The Gabor target orientation (for Detection) or the reference orientation (for Coarse and Fine Discrimination) deviated from the orientation of the unattended flickering grating by 0, 10, 20, 30, 40, or 90 degrees. Thus with increasing orientation offset either 1) the single physical target moves away from the unattended flicker orientation (during Detection), 2) one of two potential targets moves away from the unattended flicker orientation (during Coarse Discrimination), or each of the two potential targets moves away from the unattended flicker orientation (during Fine Discrimination). For example, in the 10 deg offset Detection condition the single physical target was directly offset from the unattended flicker orientation by 10 deg. During Coarse Discrimination one of the two potential targets was directly offset by 10 deg and the other target was offset by 100 deg. During Fine Discrimination the reference orientation was offset from 10 deg, and the two potential targets were offset 6 and 14 degrees from the reference. The unattended flickering grating was displayed at a fixed orientation and contrast (80%) for each subject during all EEG recording sessions (either 0 deg or 45 deg from vertical).

Threshold Procedure. An initial psychophysics session was conducted to determine the target level (i.e. the Gabor contrast) corresponding to the individuals 85% Detection and Coarse and Fine Discrimination thresholds. Individuals viewed instructions indicating which of the three tasks will be performed at the start of each block, followed by an example of the Gabor target orientation (for Detection) or the reference orientation (for Coarse and Fine Discrimination). During each trial (of a random duration uniformly distributed between 1517 and 3267 ms) individuals were instructed to use their right hand to press 'l', 'k', or 'j' to indicate if the target was present or shifted clockwise with "high", "medium", or "low" confidence, respectively. Individuals used their left hand to press 's', 'd', or 'f' to indicate if the target was absent or counterclockwise with "high", "medium", or "low" confidence, respectively. Targets appeared on 80% of the Detection trials, and the two potential targets were equally likely to appear during the Discrimination tasks. The target level presented on each trial was determined using maximum likelihood estimation (MLE) (adapted from the MLP toolbox (Grassi & Soranzo, 2009)).

The unattended flickering grating was presented in the left visual field at a fixed orientation and contrast (80 %) for each subject during all sessions (either 0 deg or 45 deg from vertical). The unattended flicker location, orientation and frequency were fixed throughout each session and served as the location, orientation and frequency in the subsequent SSVEP sessions. Subjects participated in 2 blocks of each task. The initial 15 trials of each block consisted of training with the target contrast fixed and sound feedback provided, followed by 40 threshold trials without feedback.

Separate thresholds were used Fine Discrimination since initial piloting indicated that individuals were better at fine discriminations along the meridian. Fine Discrimination threshold estimates were obtained in one block for discriminations along the vertical meridian and in the second block for the orientations away from the vertical meridian. The threshold obtained at the meridian was used as the target contrast for subsequent SSVEP trials in which the reference appeared within 10 degrees from the meridians (e.g. for the 0, 10, and 90 deg. offsets with the 0 deg. unattended grating, and for the 40 deg. offset with the 45 deg. unattended grating). The threshold away from the meridian was used for SSVEP trials at the remaining reference orientations (e.g. for 20, 30, and 40 deg. offsets with the 0 deg. unattended grating, and for the 0, 10, 20, 30, and 90 deg. offsets for the 45 deg. unattended grating).

Individuals participated in two Detection and Coarse Discrimination blocks. The target orientation (for Detection) or reference orientation (for Coarse Discrimination) was fixed within a block at either 0, 10, 30, or 40 degrees. The particular orientation offset was assigned randomly to each block. The two threshold estimates obtained for each task were averaged together, generating a single threshold estimate for Detection and a single threshold estimate for Coarse Discrimination. These thresholds were used to equate performance in the corresponding SSVEP sessions.

SSVEP Procedure. As in the threshold procedure, each SSVEP trial began with instructions to either detect a single Gabor or to discriminate between two potential gabors oriented 45 or 4 deg. cw or ccw from reference. Individuals were shown an example of the Gabor target (for Detection) or the reference orientation (for Coarse and Fine Discrimination) at high contrast, and again at their threshold contrast level. The 40 second SSVEP trial was then initiated with the onset of the flicker and individuals detected target Gabors at center and pressed a button if the target was either present (for Detection) or clockwise or counterclockwise (for Coarse and Fine Discrimination). Targets were presented randomly, but on average every 5 seconds (duration = 333 ms) within the 40 second trial. Individuals performed the same task within a single session, and each orientation was repeated 6 times per session (counterbalanced over 6 blocks in a Latin Square). The unattended flickering grating was presented in the left visual field throughout each trial.

EEG recording. EEG was recorded with a 128 channel Geodesic Sensor Net (Tucker, 1993). In order to synchronize stimulus information with EEG recording, 8 electrodes on the outer ring were disabled to record the activity of photocells placed on the monitor. An additional 10 channels on the outer ring were discarded due to a high susceptibility to muscle artifacts. The EEG signals were sampled at 1000 Hz with a 50 Hz analog low-pass filter. EEG signals were initially recorded with a vertex reference and were mathematically referenced to the average of the 110 channels for analysis. The subject's response to targets was recorded by a switch connected to the EEG system. The subject's ability to maintain fixation was monitored using an SMI eye-tracker (iView Red) camera.

SSVEP analysis. Steady-state responses to a contrast reversal flicker primarily occur at the second harmonic of the flicker frequency (Regan, 1989). Steady-state responses were estimated by decomposing each ~40 second trial of EEG recording using the discrete Fourier transform (DFT) ($\Delta f \sim .025$ Hz) implemented using the fast Fourier transform (FFT) function in MATLAB (version 7.11; The MathWorks, Natick, MA). The exact duration was an integer number of periods of the flicker. We examined the magnitude of SSVEP responses at each channel within the narrow window corresponding to the stimulus frequency by calculating the signal-to-noise ratio (SNR); the ratio of the power in the second harmonic and the average power in the 100 surrounding frequency bins (see Sutoyo & Srinivasan, 2009). SNR's were averaged over a set of 8 left parietal and 8 right parietal-temporal electrodes that captured the prominent peak SNR response within each task (see Fig 3). The overall average SNR overlaps well with the 16 electrodes that cover the peak response in individual subjects and sessions (i.e. at least one electrode overlaps within 98 out of 100 subjects/sessions).

The SNR value of the 16 electrodes was averaged to construct the individual subject SNR curves. Differences in SNR with increasing orientation offset were examined by normalizing each individual subject

SNR profile by their mean response, and conducting a one-way ANOVA with the orientation offset as the within subject variable (α=.05). Statistical tests were conducted using MATLAB subroutines (version 7.11; The MathWorks, Natick, MA). For clarity, tuning profiles are plotted after normalizing the average SNR by the SNR at zero degree off-set (indicating the percent modulation from zero) (Fig 3).

Individual Curves and Bayesian Graphical Modeling. Individual differences in attentional strategies were examined in order to determine whether different tuning profiles were related to differences in behavior, and whether individuals were able to use the optimal tuning profile across tasks. Individual differences were characterized using a hierarchical Bayesian model. The model formally "decomposes" each individual tuning curve into one of three families of circular normal (von Mises) curves constrained by either a small slope (i.e. uniform gain), a large slope and a preferred orientation around 0 deg offset (i.e. attend "on-channel"), or a large slope with a preferred orientation away from 0 deg (i.e. attend "off-channel") (see Methods and Fig. 4).

The observed SSVEP tuning profile *R* will approximate a flat line over orientations if individuals apply uniform gain. Alternatively, the response may peak at the physical target orientation if individuals enhance the gain of the physical target orientation and/or suppress the gain of orientations away from the physical targets (i.e. attention is "on-channel"). The response may peak *away* from the physical target orientation if individuals enhance the gain of neurons that code orientations away from the physical targets (i.e. if they attend "off-channel"). Each of these three potential approaches may be captured by constraining the parameters of a von Mises (circular normal) distribution: $R = \exp(\kappa \cos(\mu))$, where μ is the orientation offset between the target and the flicker orientation (here 0, 10, 20, 30, and 40 deg), and κ is a scale parameter. Constraining the function to small values of κ (e.g. $-0.01 < \kappa < 0.2$)[1] generates a family of flat curves capturing a uniform distribution of attentional gain. Restricting κ to larger values (e.g. $0.2 < \kappa < 4$) generates a family of curves with a peak response at either the physical target orientation (e.g. -15 deg $< \mu <$ 8 deg) or away from the physical target

[1] The curve is flipped along the horizontal axis when the sign of κ changes. Negative κ values help ensure that small fluctuations in a uniform responses (e.g. due to noise) are not misattributed to the "on-channel" or "off-channel" family of curves.

orientation (e.g. 8 deg < μ < 50 deg).

Bootstrap resampled SNR values were used as repeated observations in each run of the Bayesian Graphical Model, implemented in the Winbugs software (Lunn, Thomas, Best, & Spiegelhalter, 2000). SNR values were obtained for each orientation offset *i*, subject j, and bootstrapped permutation *p* (Figure 4). Specifically, Fourier analysis was conducted on the individual trials and the power values (6 for each orientation offset) were resampled and averaged to generate a single bootstrapped resampled power value for a given offset. The power values within the 100 neighboring frequency bins were also resampled and averaged, generating a bootstrapped measure of noise. The bootstrapped power corresponding to the flicker frequency was divided by the power in the surrounding frequency bins generating the SNR. One thousand posterior samples were obtained for a single run of the model with the fixed set of bootstrapped resampled SNR values.

The model was implemented repeatedly with different upper or lower boundaries for κ and μ in order to ensure that the parameter inference (i.e. the assignment to a particular family of curves) generalized over a range of parameter boundaries. The lower boundaries of κ (for the curves representing a uniform distribution of attention) were [-.04 -.03 -.02 -.01]. The upper boundary of κ values (representing the boundary between curves with a peak (i.e. "on-channel" or "off-channel") and without a peak (i.e. "uniform") were [.1 .12 .15 .2]. The upper boundary for curves with a peak was fixed for all runs at 4. The lower μ boundary (representing the boundary between the "on-channel" and "off-channel" curves) were [-25 -20 -15], while the upper boundary for μ was fixed at 50 across all runs of the model. For example, one run of the model sampled κ values continuously from the interval from [-.04 to .2] and μ values continuously from the interval from [-25 50]. The model was run using the entire 48 combinations of parameter boundaries (e.g. 4 lower κ boundaries, 4 upper κ boundaries, and 3 lower μ boundaries generate 48 combinations).

The full graphical model is displayed in Fig. 4 using plate notation (for an introduction see Shiffrin, Lee, Kim, & Wagenmakers, 2008). Each individuals group assignment is provided by the "switch" parameters

Z_{1j} and Z_{2j} which provide inference on the relative probability in which each of the three potential families may have generated the observed data. For example, on a single iteration the data may be generated by a family of uniform curves $(Z_{1j} = 1)$, or a family with peak gain at the target orientation $(Z_{1j} = 2,\ Z_{2j} = 1)$, or a family with peak gain away from the target orientation $(Z_{1j} = 2,\ Z_{2j} = 2)$. The parameters are estimated on each iteration of the Winbugs (Gibbs) sampler (1000 iterations × 48 model implementations; 500 burn-in iterations per implementation). The average value over the (48000) posterior observations captures the relative probability that the observed data belongs to each of the three families of curves. This probability was rounded to a discrete value to assign each individual to one of three families for further analysis.

Strategies and Behavioral results. The average detection or discrimination threshold (obtained at the start of the experiment) were calculated for the subset of individuals that applied each of the three different strategies for each of the three different tasks. This allowed us to examine the perceptual benefits of applying different strategies for each of the three tasks (e.g. whether individuals who apply the "optimal" strategy are better at performing the task). We identified differences in behavioral thresholds by conducting a non-parametric bootstrap analysis. (A non-parametric test was performed due to the non-normality of the threshold data (e.g. 40% (n = 40 of 100) of threshold values were at the minimum achievable contrast level of 2%). Differences in thresholds were reported if the observed difference in threshold is greater than 95% of the differences in threshold obtained after sampling randomly within each group with replacement (10000 samples) (Efron & Tibshirani, 1993).

Strategies across tasks. We examined whether individuals used a common pattern of strategies across Detection, Coarse Discrimination, and Fine Discrimination. Of particular interest was whether individuals were able to apply the optimal strategy over multiple tasks. For example, did the individuals who attended "on-channel" during Detection also attend "off-channel" during Fine Discrimination? In order to address this question we calculated the number of individuals who applied a particular pair of strategies over a pair of tasks.

This count was compared with the number of individuals who demonstrate the same pattern after permuting the subject labels for each task (with replacement).

Statistical Analysis. The subsequent analysis on the individual groups comprised a total of 9 statistical tests. Six statistical tests were conducted comparing differences in behavioral thresholds for individuals assigned to different families of curves. For example, we examined whether individuals assigned to the "on-channel" curves had lower detection thresholds than those assigned to "uniform" or "off-channel" during both Course Discrimination, and Detection, and we examined whether individuals assigned to "off-channel" curves during Fine Discrimination has lower detection thresholds than those assigned to "uniform" or "on-channel". An additional three statistical tests were performed in examining the flexibility in which individuals directed attention across the tasks. This consisted of a statistical interaction between task and orientation and two bootstrap tests examining whether a significant number of individuals assigned to the "off-channel" curves for Fine Discrimination and "on-channel" curves for either Detection or Course Discrimination. Eight out of 9 of the a priori tests were significant at an uncorrected threshold of $p < .05$. Two out of the 9 tests are significant after Holm-Bonferroni correction for multiple comparisons (with $p < .0021$ and $p < .0034$).

Results

Behavior. The average 85% thresholds were 3.6 for Detection (D) (SE = .49) (n=33), 6.0 for Coarse Discrimination (CD) (SE = 1.39) (n=34), and 15.3 for Fine Discrimination (FD) (SE = 1.12) (n=33). The average hit rate in the subsequent SSVEP experiment was 80.2, 82.7, and 68.3% correct for Detection, Coarse Discrimination, and Fine Discrimination, respectively. The hit rate and false alarm rate in the SSVEP experiment were combined to generate A', a nonparametric measure of perceptual sensitivity (See, Warm, Dember, & Howe, 1997; Stanislaw & Todorov, 1999) for each task and orientation offset. A two-way repeated measures ANOVA was conducted for the 32 subjects that participated in all conditions, with the factors 'task' (D, CD, or FD) and 'orientation-offset' (0, 10, 20, 30, or 40 deg.). We found no significant differences in log(A') with increasing orientation offset ($F(4,124) = 1.11$, $p = .35$), or across tasks ($F(2,62) = 1.41$, $p = .25$) and an interaction between 'task' and 'orientation offset' ($F(8,248) = 2.22$, $p = .03$).

Attentional tuning curves (SSVEP responses over orientation). The SNR of the SSVEP response was measured while individuals detected targets that overlapped with the flicker orientation by 0, 10, 20, 30, 40, and 90 deg. We anticipated that the maximum SNR will be observed when the flicker orientation aligns with the peak of the attentional tuning function. We found a monotonic decline in the signal-to-noise ratio (SNR) with increasing orientation offset during Detection and Fine Discrimination from 0 deg to 30 deg offsets (Fig. 3). The decline from 0 to 30 deg. was more pronounced during Detection, with a maximum percent reduction in SNR (from 0 deg) of 6.0% when the target orientation was offset from the flicker orientation by 30 deg (compared to 2.9% for Fine Discrimination and 1.9% for Coarse Discrimination at 40 deg). Despite the trend in which responses to the unattended flicker are reduced with increasing offset (e.g. the majority of points falling below 1 in figure 3) a one-way ANOVA revealed no significant differences in SNR with orientation for each of the three tasks ([$F(5,192) = 1.49$; $p = .194$], [$F(5,198) = 0.36$; $p = .874$], [$F(5,192) = 1.67$; $p = .144$], for D, CD, and FD, respectively).

The absence of robust differences at the group level may be due to a number of factors that can contribute variance to the SSVEP curves. For example, attentional gain may be less spatially widespread in some subjects and may depend on task difficulty. In addition, the horizontal unattended flicker may have sampled a larger population of neurons than the oblique flicker, individuals may have utilized a mixture of strategies within a task, and there may be individual differences in attention strategies within detection and fine and coarse discriminations. The subsequent analysis focuses on the contribution of individual differences by examining whether SSVEP curves are related to perceptual performance, and whether individuals can flexibly apply different strategies over different tasks.

Evaluating attentional strategies and behavior. Individual differences in attention strategies were characterized using a hierarchical Bayesian model. We found that 26, 33, and 41% of the sessions (e.g. tasks and individuals) were assigned to uniform, "on-channel", and "off-channel" respectively. The individual average mean (μ) and scale (κ) parameters are indicated in Figure 5.

The individual assignments to "uniform", "on-channel" and "off-channel" were determined based upon the entire dataset, as described in the methods. We verified that these assignments would generalize to data that wasn't included in the model by dividing the data in half into a training and test data set. The Bayesian Model Estimation was conducted identically as before on the training set, and then the average SNR was obtained with the test data for each subject. Subject assignments were determined for the test data set by finding the family of curves (e.g. the uniform, "on-channel" and "off-channel" curves) which best fit the average SNR of the test data. We found 78% agreement between the assignments from the training and the test data. In addition, the average curve within the test data demonstrated the pattern of modulation suggested by the training data. For example, the individuals assigned to "on-channel" with the training data demonstrated the largest average response at 0 deg. orientation offset within the test data, while the individuals assigned to "off-channel" with the training data demonstrated the largest average response at the 20 deg. orientation offset in the test data.

It is likely that different attentional strategies are associated with differences in perceptual performance. For example, individuals with enhanced responses to the target orientation (i.e. those with "on-channel" curves) may contain an enhanced perceptual representation of the target. This enhanced perceptual representation may manifest as a reduction in detection/discrimination thresholds within the individuals who attend "on-channel" during Detection and Coarse Discrimination (Regan & Beverley, 1985). Alternatively, individuals with enhanced responses within "off-channel" neurons may be better at discriminating nearby orientations. This result would be consistent with the account that "off-channel" neurons provide the most relevant information for fine discrimination (Jazayeri & Movshon, 2006; Navalpakkam & Itti, 2007; Scolari et al., 2012; Scolari & Serences, 2009).

We observed the lowest thresholds for individuals with “on-channel” curves during Detection and Coarse Discrimination (mean % contrast: 2.68 and 2.83, respectively). In each case, the threshold was lower than the threshold of the group that applied uniform gain ([difference in % contrast: 1.15; CI: [-0.02 3.18] ; p = .0267], and [difference in % contrast: 6.92; CI: [-2.80 10.24]; p = .0362]). During Fine Discrimination, the lowest thresholds were observed for the individuals with “off-channel” curves, (mean % contrast: 12.51), followed by “on-channel” (mean % contrast: 15.45) and “uniform” (mean % contrast: 21.78). The groups with “off-channel” and “on-channel” curves had significantly lower thresholds than the group with uniform curves (difference in % contrast: 9.27; CI: [4.10 14.07]; p = .0034; difference in % contrast: 6.32; CI: [2.49 11.69]; 5.64; p = .0442) (see Fig. 6). Thus the results suggest that during each of the three tasks the individuals who attended “on-channel” had significantly lower thresholds than the individuals who applied uniform gain. Individuals who attended “off-channel” additionally have significantly lower thresholds (than the individuals that applied uniform gain) during Fine Discrimination.

Evaluating the flexibility of attentional strategies. We next examined whether individuals applied a common pattern of strategies across a pair of tasks. Specifically, we were interested in whether individuals who were assigned to the optimal family of curves during Detection or Coarse Discrimination (e.g. “on-channel”) were also assigned to the optimal family of curves during Fine Discrimination (e.g. “off-channel”). Non-parametric bootstrap tests (10000 samples) revealed that a significant subset of individuals attended “on-channel” during Detection and “off-channel” during Fine Discrimination (N = 8; p = .0125). The number of individuals who apply a pattern of curves over tasks is demonstrated in Fig. 7. Figure 8 demonstrates the topographic distribution of SNR responses for an individual with an on-channel curve for Detection and an off-channel curve for Fine Discrimination.

In order to examine this pattern further, we took the subset of individuals assigned to a particular curve during one task, and examined their average percent modulation in each of the other two tasks. Significant differences in strategies across tasks were investigated by examining the interaction between "task" and "orientation" in a two-way ANOVA with the percent modulation (from mean SNR) as the dependent variable. There was a significant interaction between "task" and "orientation" for the subset of individuals assigned to "off-channel" curves during Fine Discrimination (in Fig. 9) ($F(10,216) = 2.88$, $p = .0021$). The interaction approached significance for the subset of individuals assigned to "on-channel" curves during Fine Discrimination (in Fig. 9) ($F(10,180) = 1.84$, $p = .0571$). The individuals assigned to the "on-channel" curves during Fine Discrimination demonstrate a similar pattern of responses for Coarse Discrimination but a more uniform pattern of responses during Detection. The individuals assigned to the "off-channel" curves during Fine Discrimination show a reduced SNR from 0 to 30 degree offsets (Fig. 9) for Detection. This pattern likely contributed to the observed interaction and is consistent with the finding that a significant number of individuals attend "off-channel" during Fine Discrimination and "on-channel" during Detection.

Discussion

Psychophysical studies suggest that neurons coding "off-channel" orientations are most informative during fine discriminations (Hol & Treue, 2001; Regan & Beverley, 1985; Scolari & Serences, 2009; Wilson & Regan, 1984). Bold fMRI studies further demonstrate that "off-channel" activity within early sensory areas is predictive of subsequent fine discrimination performance (Scolari et al., 2012; Scolari & Serences, 2010). The present study extends these results using a novel technique that aims to measure attentional tuning profiles within frequency tagged cortical networks. We found considerable individual variability in the tuning curves during Detection, Coarse and Fine Discrimination tasks. Decomposing tuning profiles into "on-channel" "off-channel" and uniform strategies with Bayesian modeling allowed us to characterize these individual differences according to their relation with behavioral performance and their distribution across tasks.

We found that the individuals with "on-channel" curves had significantly lower detection and discrimination thresholds for each of the three tasks compared to the individuals with uniform curves. During

Fine Discrimination we also found that the individuals with “off-channel” curves had significantly lower discrimination thresholds than the individuals with uniform curves. These results suggest that there are perceptual benefits to enhancing the gain of neurons coding the physical features of target stimuli during detection and fine and coarse discrimination tasks. The additional presence of significantly lower thresholds for individuals attending “off-channel” during Fine Discrimination is consistent with previous studies demonstrating that fine discrimination encourages enhancing the gain of neurons coding orientations slightly offset from the target orientation. Collectively, the results add to the growing body of literature indicating that individuals can apply gain in an optimal manner, and demonstrate that differences in gain are functionally related to differences in behavioral performance.

Individuals are theoretically motivated to distribute attentional gain in different ways over each of the three tasks. The distribution of attentional gain differs in terms of the optimal place to apply peak gain (e.g. “on-channel” during Detection but “off-channel” during Fine Discrimination) and the complexity of attentional tuning (e.g. one peak for Detection compared to two peaks for Discrimination). Applying the optimal strategy across each of these tasks encourages individuals to shape their attentional tuning in a relatively flexible manner. We examined the number of individuals who applied a particular pattern of strategies across two tasks and found that a significant number of individuals demonstrate “on-channel” curves during Detection and “off-channel” curves during Fine Discrimination. These results suggest that there are only a subset of individuals who apply the optimal strategy in the context of detection and fine discriminations.

The present tuning profiles are reflected within cortical networks targeted with the steady-state visual evoked potential (SSVEP). In contrast, previous findings on the influence of attention on sensory gain have been largely restricted to early sensory areas that are robustly tuned to the stimulus feature. These constraints arise due to both the innate differences in the neural sensitivity to stimulus features, as well as due to the particulars of the recording technique. For example, single unit studies demonstrate that orientation tuning curves may be measured over a series of anatomically and functionally isolated visual areas (e.g. V1, V2, and V4), and the degree of attentional modulation is increased within areas with more complex stimulus-response properties (e.g. V4 vs. V1) (McAdams & Maunsell, 1999). The single unit dynamics captured by electrophysiological recordings are not captured by the comparatively lower spatial resolution of the BOLD fMRI voxel, however, recent techniques demonstrate that orientation information may be extracted at least in area V1, which contains a high density of orientation selective cells (Haynes & Rees, 2005; Kamitani & Tong, 2005; Serences, Saproo, Scolari, Ho, & Muftuler, 2009).

The frequency tagging technique provides the opportunity to isolate cortical activity that is time-locked to a periodic visual input with a fixed orientation. Thus, while EEG is incapable of measuring the orientation profile of individual neurons, it is a promising method to monitor the activity of cortical networks that entrain with neurons sensitive to the flicker orientation. Enhanced gain within early sensory areas is well posed to propagate to brain networks that synchronize with the periodic visual input. Thus, a unique contribution of the frequency tagging technique is that it can potentially provide a measure of the response to basic visual features beyond the earliest stages of visual processing. However, further studies are required to determine precisely how the frequency tagged network activity in the current study is related to activity within the early sensory areas traditionally examined with single unit and BOLD fMRI measures.

It is important to note that the individual tuning profiles in the current study were measured by isolating the SSVEP response to an *unattended* flicker. Thus, the experimental design leverages upon the phenomenon that attending to a feature at one location also results in an enhanced response to that feature within neurons or voxels sensitive to unattended spatial locations (Bichot, 2005; Martinez-Trujillo & Treue, 2004; Saenz et al., 2002; Serences & Boynton, 2007; Treue & Martinez-Trujillo, 1999). Within this context, the unattended flicker may serve as a “probe” to measure the attentional strategy applied at the attended spatial location. Previous studies examining the influence of “off-channel” attentional gain have focused on neurons that code the attended regions of the visual display. Thus, as far as we are aware, the present study is the first to explicitly examine whether "off-channel" gain also extends to neurons coding unattended regions of the visual field, and the implication of their attentional profile on visual perception and attention strategies applied over different tasks.

Conclusion

Individuals tuning curves were examined by measuring the SSVEP response to a fixed orientation while individuals attended to a range of orientations during Detection, Coarse Discrimination, and Fine Discrimination tasks. There were no statistical differences in the overall tuning profile across the three tasks. The absence of robust effects may result in part due to variability in individual attention strategies as suggested by the relationship between SSVEP curves and perceptual performance and the relationship of SSVEP curves across tasks. Individuals with tuning curves centered on the physical target orientation (i.e. "on-channel") had significantly lower detection/discrimination thresholds then those with uniform curves. Individuals with curves that peak away from the target orientation during Fine Discrimination additionally demonstrate significantly lower discrimination thresholds (than those who apply uniform gain). This emphasizes the perceptual benefits of attending "off-channel" during fine discriminations. Further, a significant subset of the individuals apply "on-channel" attentional tuning during Detection and "off-channel" tuning during Fine Discrimination. This demonstrates that some individuals may flexibly and optimally apply attention during detection and fine discrimination.

Grants

This work was supported by NIH grant 2 R01 MH68004.

Acknowledgments

We would like to thank Barbara Dosher, George Sperling, and Michael Lee for helpful comments.

References

Bichot NP. Parallel and Serial Neural Mechanisms for Visual Search in Macaque Area V4. *Science 308*(5721); 529–534, 2005.

Bisley JW. Neuronal Activity in the Lateral Intraparietal Area and Spatial Attention. *Science 299*(5603): 81–86, 2003.

Brainard DH. The psychophysics toolbox. *Spatial vision 10*(4): 433–436, 1997.

Bridwell DA, Srinivasan R. Distinct attention networks for feature enhancement and suppression in vision. *Psychological Science* 23(10):1151-1158, 2012.

Cohen MR, Maunsell JHR. Using Neuronal Populations to Study the Mechanisms Underlying Spatial and Feature Attention. *Neuron 70*(6): 1192–1204, 2011

Corbetta M, Patel G, Shulman GL. The Reorienting System of the Human Brain: From Environment to Theory of Mind. *Neuron 58*(3): 306–324, 2008

Corbetta M, Shulman GL. Control of goal-directed and stimulus-driven attention in the brain. *Nature Reviews Neuroscience 3*(3): 215–229, 2002.

Crapse TB, Sommer MA. Frontal eye field neurons with spatial representations predicted by their subcortical input. *The Journal of Neuroscience 29*(16): 5308–5318, 2009.

Efron B, Tibshirani R. *An introduction to the bootstrap*. Chapman and Hall, 1993.

Fanini A, Assad JA. Direction Selectivity of Neurons in the Macaque Lateral Intraparietal Area. *Journal of Neurophysiology 101*(1): 289–305, 2008.

Freedman DJ, Assad JA. Experience-dependent representation of visual categories in parietal cortex. *Nature 443*(7107): 85–88, 2006.

Grassi M, Soranzo A. MLP: A MATLAB toolbox for rapid and reliable auditory threshold estimation. *Behavior research methods 41*(1): 20–28, 2009.

Gregoriou GG, Gotts SJ, Zhou H, Desimone R. Long-range neural coupling through synchronization with attention. *Progress in Brain Research* 176:, 35–45, 2009.

Haenny P, Schiller P. State dependent activity in monkey visual cortex. *Experimental Brain Research 69*(2): 225–244, 1988.

Haynes J-D, Rees G. Predicting the orientation of invisible stimuli from activity in human primary visual cortex. *Nature Neuroscience 8*(5): 686–691, 2005.

Hol K, Treue S. Different populations of neurons contribute to the detection and discrimination of visual motion. *Vision Research 41*(6): 685–689, 2001

Jazayeri M, Movshon JA. Optimal representation of sensory information by neural populations. *Nature Neuroscience 9*(5): 690–696, 2006.

Kamitani Y, Tong F. Decoding the visual and subjective contents of the human brain. *Nature Neuroscience 8*(5): 679–685, 2005.

Liu T, Hospadaruk L, Zhu DC, Gardner JL. Feature-specific attentional priority signals in human cortex. *The Journal of Neuroscience 31*(12): 4484–4495, 2011.

Lunn DJ, Thomas A, Best N, Spiegelhalter D. WinBUGS-a Bayesian modelling framework: concepts, structure, and extensibility. *Statistics and computing 10*(4): 325–337, 2000.

Martinez-Trujillo JC, Treue S. Feature-based attention increases the selectivity of population responses in primate visual cortex. *Current Biology 14*(9): 744–751, 2004.

Maunsell JH, Sclar G, Nealey TA, DePriest DD. Extraretinal representations in area V4 in the macaque monkey. *Visual Neuroscience 7*(6): 561–573, 2001.

McAdams, CJ, Maunsell JH. Effects of attention on orientation-tuning functions of single neurons in macaque cortical area V4. *The Journal of Neuroscience 19*(1): 431–441, 1999.

Moore T, Fallah M. Control of eye movements and spatial attention. *Proceedings of the National Academy of Sciences 98*(3): 1273, 2001

Motter BC. Focal attention produces spatially selective processing in visual cortical areas V1, V2, and V4 in the presence of competing stimuli. *Journal of Neurophysiology 70*(3): 909–919, 2003.

Motter BC. Neural correlates of attentive selection for color or luminance in extrastriate area V4. *The Journal of Neuroscience 14*(4): 2178–2189, 1994.

Navalpakkam V, Itti L. Search Goal Tunes Visual Features Optimally. *Neuron 53*(4): 605–617, 2007.

Nunez P, Srinivasan R. *Electric Fields of the Brain: The neurophysics of EEG (2nd ed.)*. New York: Oxford University Press, 2006.

Pelli DG. The VideoToolbox software for visual psychophysics: transforming numbers into movies. *Spatial Vision 10*(4): 437–442, 1997.

Purushothaman G, Bradley DC. Neural population code for fine perceptual decisions in area MT. *Nature Neuroscience 8*(1): 99–106, 2005.

Raiguel S, Vogels R, Mysore SG, Orban GA. Learning to see the difference specifically alters the most informative V4 neurons. *The Journal of neuroscience 26*(24): 6589, 2006.

Regan D. *Human Brian Electrophysiology: Evoked potentials and evoked magnatic fields in science and medicine*. New York: Elsevier, 1989.

Regan D, Beverley KI. Postadaptation orientation discrimination. *Journal of the Optical Society of America A 2*(2): 147–155, 1985.

Saenz M, Buracas GT, Boynton GM. Global effects of feature-based attention in human visual cortex. *Nature Neuroscience 5*(7): 631–632, 2002.

Schoups A, Vogels R, Qian N, Orban G. Practicing orientation identification improves orientation coding in V1 neurons. *Nature* 412(6846): 549–553, 2001.

Scolari M, Byers A, Serences JT. Optimal deployment of attention gain during fine discriminations. *Journal of Neuroscience* 32(22): 7723-7733, 2012

Scolari M, Serences JT. Adaptive allocation of attentional gain. *The Journal of Neuroscience 29*(38): 11933–11942, 2009.

Scolari M, Serences JT. Basing Perceptual Decisions on the Most Informative Sensory Neurons. *Journal of Neurophysiology 104*(4): 2266–2273, 2010.

See JE, Warm JS, Dember WN, Howe SR. Vigilance and signal detection theory: An empirical evaluation of five measures of response bias. *Human Factors 39*(1): 14–29, 1997.

Serences JT, Saproo S, Scolari M, Ho T, Muftuler LT. Estimating the influence of attention on population codes in human visual cortex using voxel-based tuning functions. *Neuroimage 44*(1): 223–231, 2009.

Serences JT, Yantis S. Selective visual attention and perceptual coherence. *Trends in Cognitive Sciences 10*(1): 38–45, 2006.

Serences JT, Boynton GM. Feature-based attentional modulations in the absence of direct visual stimulation. *Neuron* 55(2): 301–312, 2007.

Shiffrin RM, Lee MD, Kim W, Wagenmakers EJ. A survey of model evaluation approaches with a tutorial on hierarchical Bayesian methods. *Cognitive Science 32*(8): 1248–1284, 2008.

Stanislaw H, Todorov N. Calculation of signal detection theory measures. *Behavior Research Methods, Instruments & Computers 31*(1): 137–149, 1999.

Stokes M, Thompson R, Nobre AC, Duncan J. Shape-specific preparatory activity mediates attention to targets in human visual cortex. *Proceedings of the National Academy of Sciences 106*(46): 19569, 2009.

Sutoyo D, Srinivasan R. Nonlinear SSVEP responses are sensitive to the perceptual binding of visual hemifields during conventional “eye” rivalry and interocular “percept” rivalry. *Brain research* 1251: 245–255, 2009.

Treue S, Martinez-Trujillo JC. Feature-based attention influences motion processing gain in macaque visual cortex. *Nature* 399: 575–579, 1999.

Verghese P, Kim JY, Wade AR. Attention selects informative neural populations in human V1. *Journal of Neuroscience* 32(46):16379-16390, 2012.

Wilson HR, Regan D. Spatial-frequency adaptation and grating discrimination: predictions of a line-element model. *Journal of the Optical Society of America A* 1; 1091–1096, 1984.

Figure Legends

Figure 1. Example stimuli and experimental timeline. Example stimuli are shown for each task for the 0 deg and 20 deg offset. Target Gabors are displayed at fixation and the peripheral flicker (square wave) is displayed in the left visual field at a fixed orientation. Individuals detected a single Gabor patch of known orientation (Detection, a), or discriminated between two potential Gabor's oriented either 45 degrees clockwise (cw) or counterclockwise (ccw) from reference (Coarse Discrimination, b), or 4 degree cw or ccw from reference (Fine Discrimination, c). An example timeline is shown in (d) for the 0 degree offset for each of the three tasks. Eight targets appeared on average within the 40 s SSVEP trial. Target Gabors are indicated by each tick and the Gabor orientation is indicated above. In addition to 0 and 20 degrees, SSVEP responses were also measured at 10, 30, 40, and 90 degree offsets.

Figure 2. Predicted SSVEP responses. Individuals likely apply gain to neurons coding the most informative information during each of the three tasks. These "optimal" attentional gain functions are depicted for targets that are offset by 0 and 20 degrees from the unattended grating orientation (left column) for Detection (a), Coarse Discrimination (b), and Fine Discrimination (c). Changing the orientation of the target Gabor shifts the attentional gain function. Attentional gain also extends to neurons that code unattended regions, thus the SSVEP response to the unattended grating (of *fixed* orientation) may be shaped by (and reflect) attentional gain at the attended region. The predicted response for the 0 and 20 degree offsets are indicated by the two dots on the

right column for the corresponding task. The full predicted SSVEP response over a range of target orientations is indicated on the right, where the two dots on the curve correspond to measurements obtained for the 0 and 20 degree offsets. Given these underlying attentional gain functions, we predict similar SSVEP modulations during Detection and Coarse Discrimination. In contrast, if individuals apply gain toward "off-channel" orientations during Fine Discrimination, then an increased SSVEP response should be observed as the target orientations move away from the grating orientation (c).

Figure 3. Average SSVEP response. The percent change in the average SNR of the SSVEP response is indicated for Detection (n=33), Coarse Discrimination (n=34), and Fine Discrimination (n=33) in a. In general, the response to the unattended flicker is reduced as the target orientation is offset from the flicker orientation by 0, 10, 20, 30, and 40 degrees. This decline is especially prominent for Detection, slightly less pronounced with Fine Discrimination, and considerably less pronounced with Coarse Discrimination. Error bars represent +/- 1 SE. The topographic plots (b) indicate the average SNR within each task, collapsed across subjects and orientations (n=198, 204, and 198, respectively). The SNR was averaged over the two patches of electrodes (in white) in the analysis for each task. Large gray electrodes mark the 10-20 placements that correspond (from bottom to top) to occipital, parietal, central, frontal, and prefrontal brain locations.

Figure 4. Bayesian Graphical Model. The observed SSVEP response R with orientation offsets i = 0, 10, 20, 30, and 40 was characterized by a Von Mises distribution for each individual j = 1, … ns (ns = total individuals) and bootstrapped observation p = 1, … np. The observed response is generated from one of three potential families of curves, which are formally described by restricting the prior distribution of κ, the scale parameter and μ, the preferred orientation. Draws from the prior distributions are shown for each of the three families above the graphical model. The binary variable Z_{1j} assigns observed data to the family of uniform curves (left)

or a family of curves that peak. The binary variable Z_{2j} assigns the observed data to the family of curves with a peak at the target orientation (attend "on-channel", $Z_{2j} = 1$) or away from the target orientation (attend "off-channel", $Z_{2j} = 2$).

Figure 5. Individual Parameter Estimates. The average μ (preferred orientation) and κ (slope) estimates are indicated for the subjects assigned to the uniform, on-channel and off-channel family of curves. The lines denote the approximate boundaries between the uniform, the on-channel and the off-channel curves.

Figure 6. Individual differences. Discrimination or detection thresholds are shown for each task separately for individuals assigned to each of the three strategies (e.g. those who apply uniform gain, attend "on-channel", or attend "off-channel"). During Detection (a), Coarse Discrimination (b), and Fine Discrimination (c) individuals who attended to the target orientation have significantly lower detection thresholds than those who apply uniform gain. During Fine Discrimination (c) individuals who attend "off-channel" additionally show significantly lower thresholds than those who apply uniform gain. The mean threshold (% contrast) is indicated by the white line in the middle of each box. The boundaries of the box indicate the lower and upper quartiles, and the lower and upper whiskers indicate the 5th and 95th percentile of the bootstrap samples, respectively.

Figure 7. The full distribution of curves. A dot is placed above a column for each individual that demonstrates the corresponding pattern of tuning curves across two tasks. The pattern of curves is demonstrated for Fine Discrimination and Detection (a), Fine Discrimination and Coarse Discrimination (b) and Coarse Discrimination and Detection (c). For example, the column with eight dots in a indicates the eight individuals with "off-channel" curves during Fine Discrimination and "on-channel" curves during Detection.

Figure 8. Individual subject SNR for each task. The topographic distribution of an individual subjects average SNR is indicated for Detection, Coarse Discrimination, and Fine Discrimination. The results are shown for orientation offsets of 0 deg., 10 deg., 20 deg., 30 deg., and 40 deg. The individual was assigned to the on-channel family of curves for Detection and the off-channel family of curves for Coarse Discrimination and Fine Discrimination.

Figure 9. Attention strategies across tasks. The average percent modulation of SNR (from zero) is shown (on the left) for the subset of individuals who attended "off-channel" during Fine Discrimination (light gray) along with the percent modulation when the same subset of individuals performed Detection (black) and Coarse Discrimination (dark gray). The average percent modulation for individuals who attend "on-channel" during Fine Discrimination is shown on the right along with their average percent modulation during Detection (black) and Coarse Discrimination (dark gray). Error bars represent +/- 1 SE.

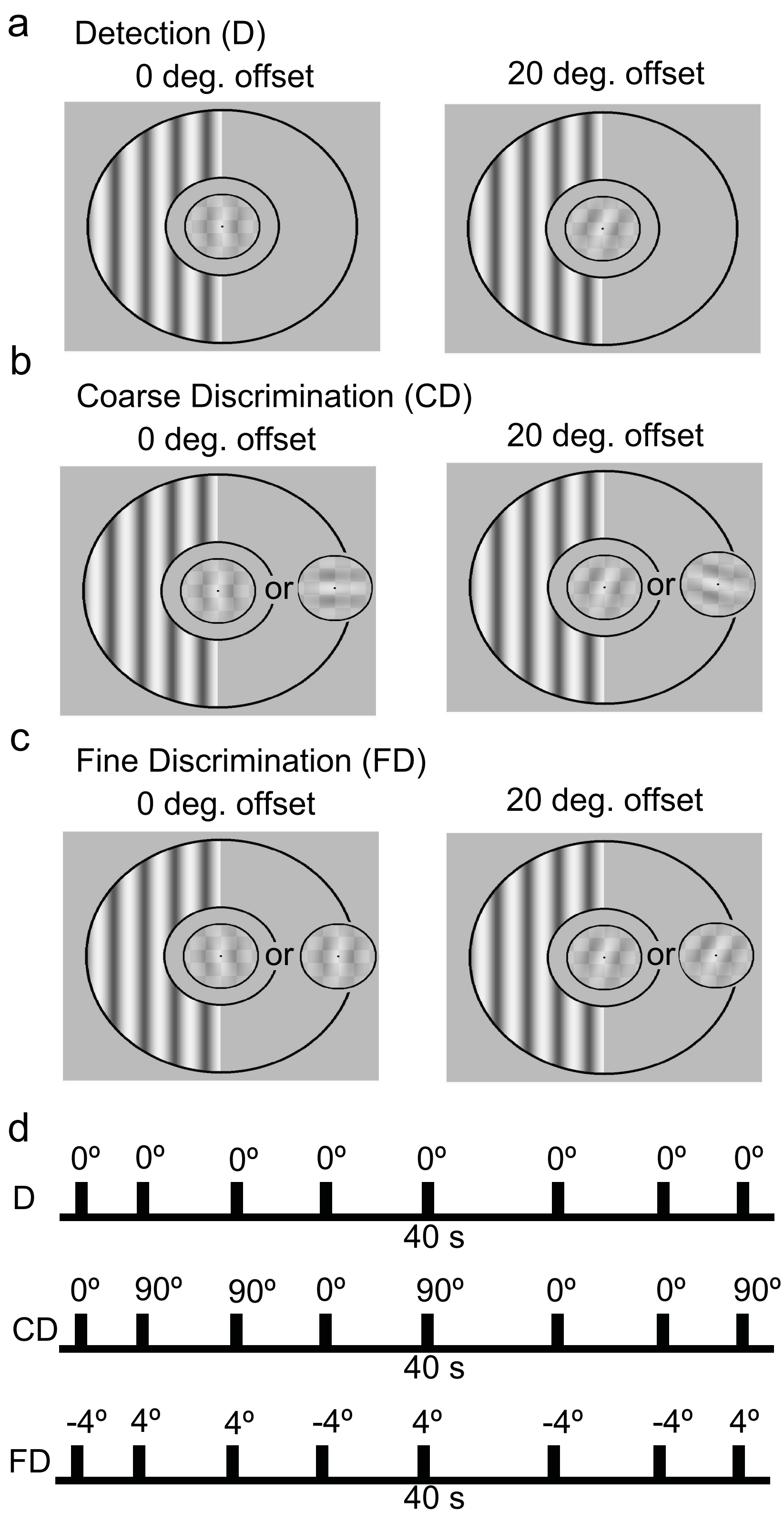
a
Detection (D)
0 deg. offset
20 deg. offset
b
Coarse Discrimination (CD)
0 deg. offset
or
20 deg. offset
or
c
Fine Discrimination (FD)
0 deg. offset
or
20 deg. offset
or
d
D
0º 0º 0º 0º 0º 0º 0º 0º
40 s
CD
0º 90º 90º 0º 90º 0º 0º 90º
40 s
FD
-4º 4º 4º -4º 4º -4º -4º 4º
40 s

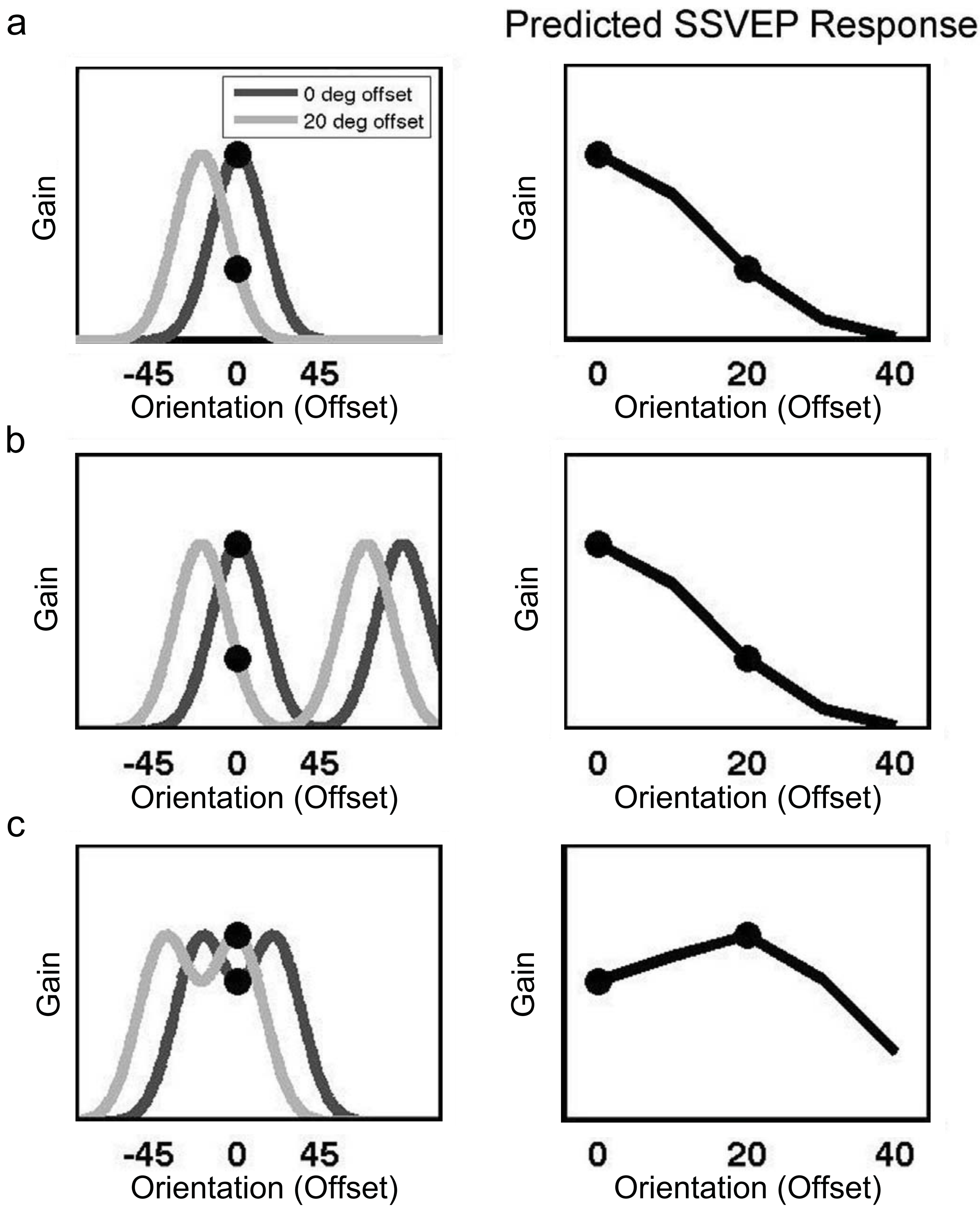

a
Predicted SSVEP Response
0 deg offset
20 deg offset
Gain
-45
0
45
Orientation (Offset)
Gain
0
20
40
Orientation (Offset)
b
Gain
-45
0
45
Orientation (Offset)
Gain
0
20
40
Orientation (Offset)
c
Gain
-45
0
45
Orientation (Offset)
Gain
0
20
40
Orientation (Offset)

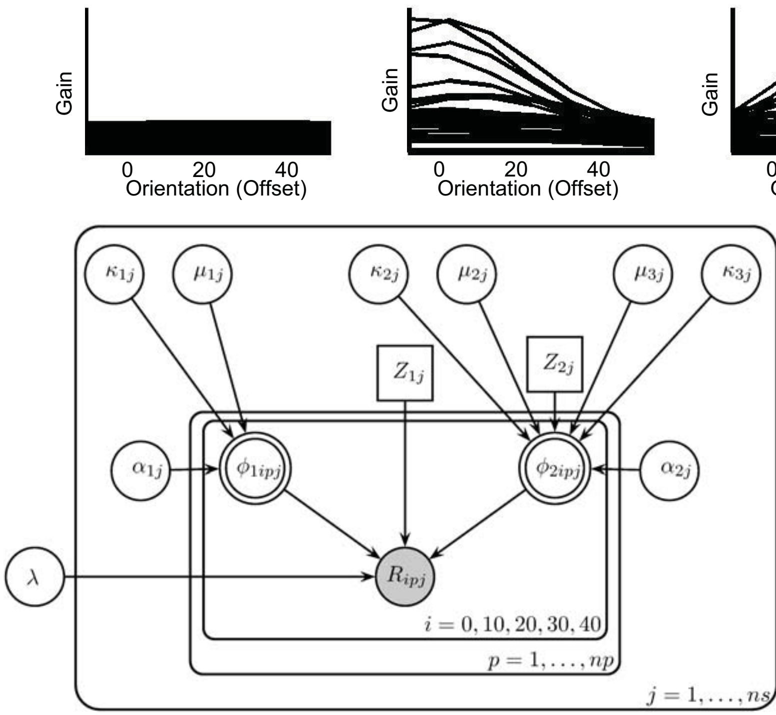

$$\mu_{2j} \sim \text{Uniform}(-15, 8)$$
$$Z_{2j} \sim \text{Bernoulli}(1/2)$$
$$\mu_{3j} \sim \text{Uniform}(8, 50)$$
$$\kappa_{2,3j} \sim \text{Uniform}(.2, 4)$$
$$\alpha_{2j} \sim \text{Uniform}(0, 40)$$
$$\phi_{2ipj} = \text{vonMises}(\mu_{Z_{2j}}, \kappa_{Z_{2j}}, \alpha_{2j})$$
$$Z_{1j} \sim \text{Bernoulli}(1/2)$$
$$\mu_{1j} \sim \text{Uniform}(-15, 50)$$
$$\kappa_{1j} \sim \text{Uniform}(-.2, .2)$$
$$\alpha_{1j} \sim \text{Uniform}(0, 40)$$
$$\phi_{1ipj} = \text{vonMises}(\mu_1, \kappa_1, \alpha_{1j})$$
$$R_{Z_{1j}ipj} \sim \text{Gaussian}(\phi_{Z_{1j}ipj}, \lambda = 1000)$$

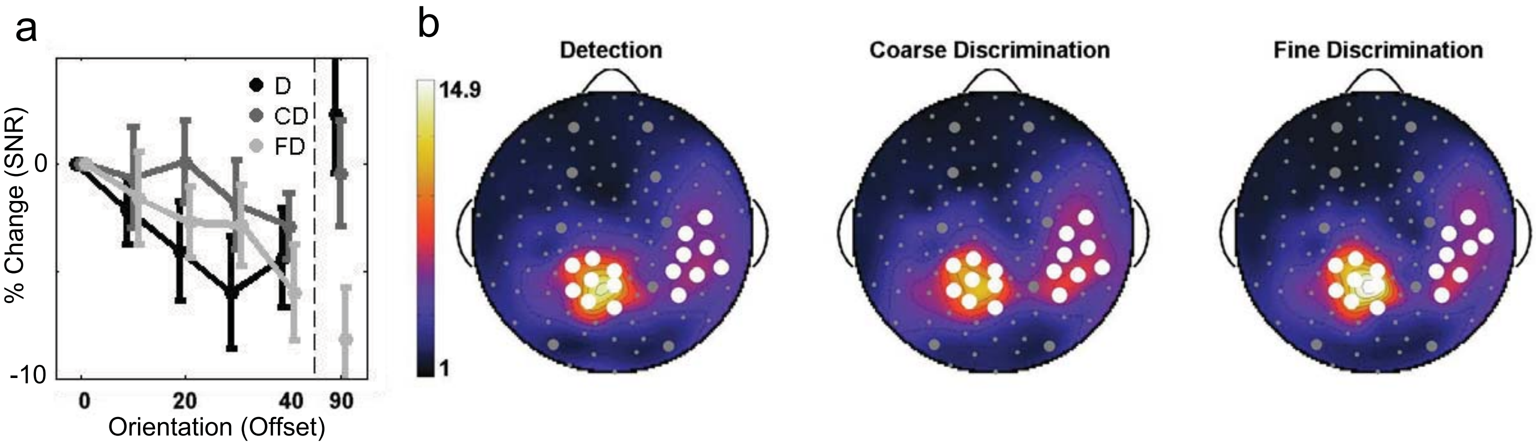
a
D
CD
FD
% Change (SNR)
0
-10
0
20
40
90
Orientation (Offset)
b
Detection
Coarse Discrimination
Fine Discrimination
14.9
1

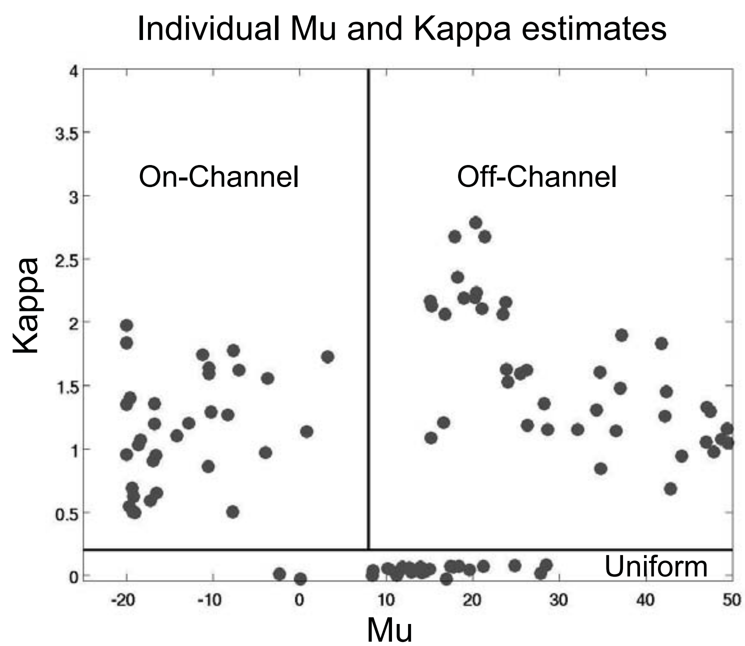
Individual Mu and Kappa estimates
On-Channel
Off-Channel
Uniform
Kappa
Mu
0
0.5
1
1.5
2
2.5
3
3.5
4
-20
-10
0
10
20
30
40
50

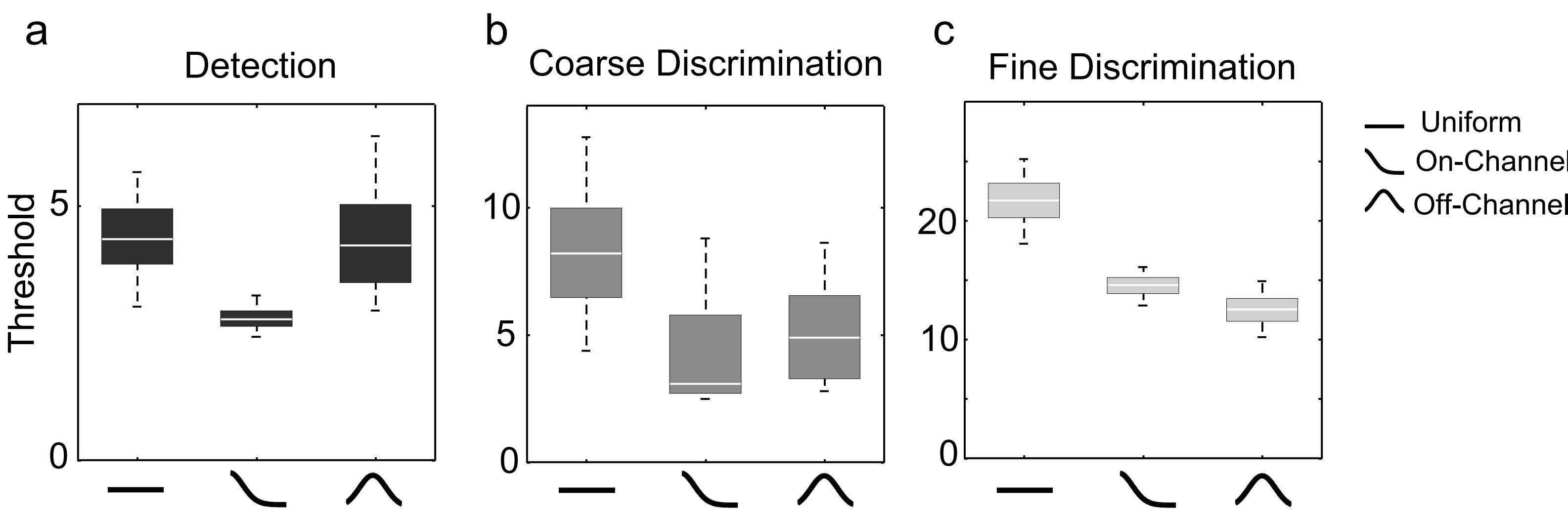

a
Detection
b
Coarse Discrimination
c
Fine Discrimination
Threshold
0
5
0
5
10
0
10
20
Uniform
On-Channel
Off-Channel

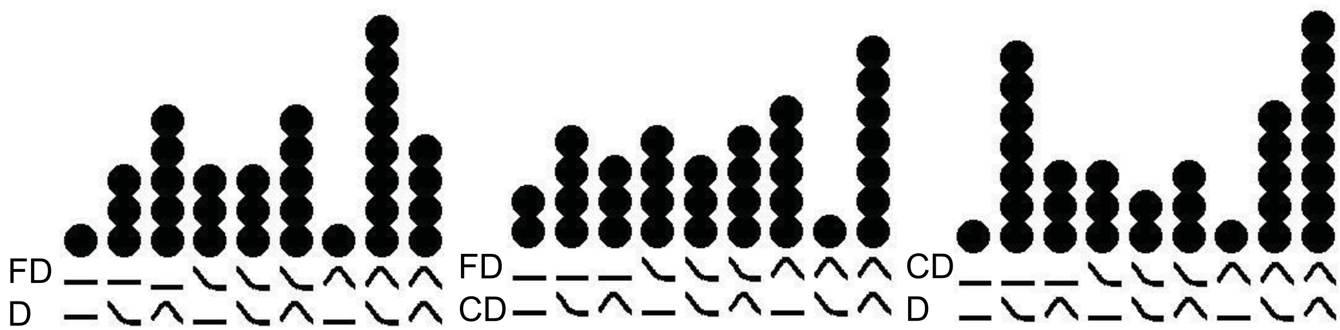
FD
D
FD
CD
CD
D

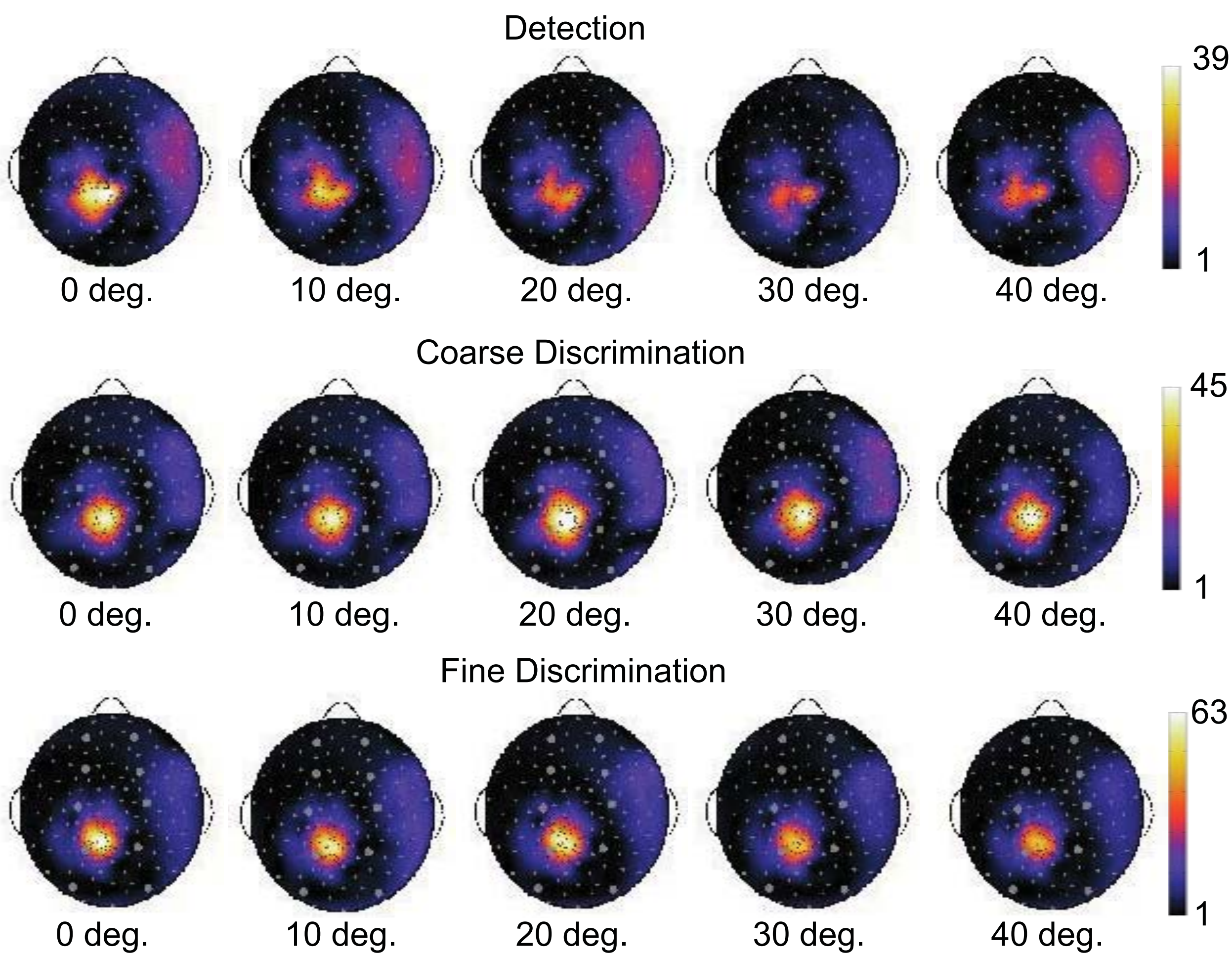
Detection
39
1
0 deg.
10 deg.
20 deg.
30 deg.
40 deg.
Coarse Discrimination
45
1
0 deg.
10 deg.
20 deg.
30 deg.
40 deg.
Fine Discrimination
63
1
0 deg.
10 deg.
20 deg.
30 deg.
40 deg.

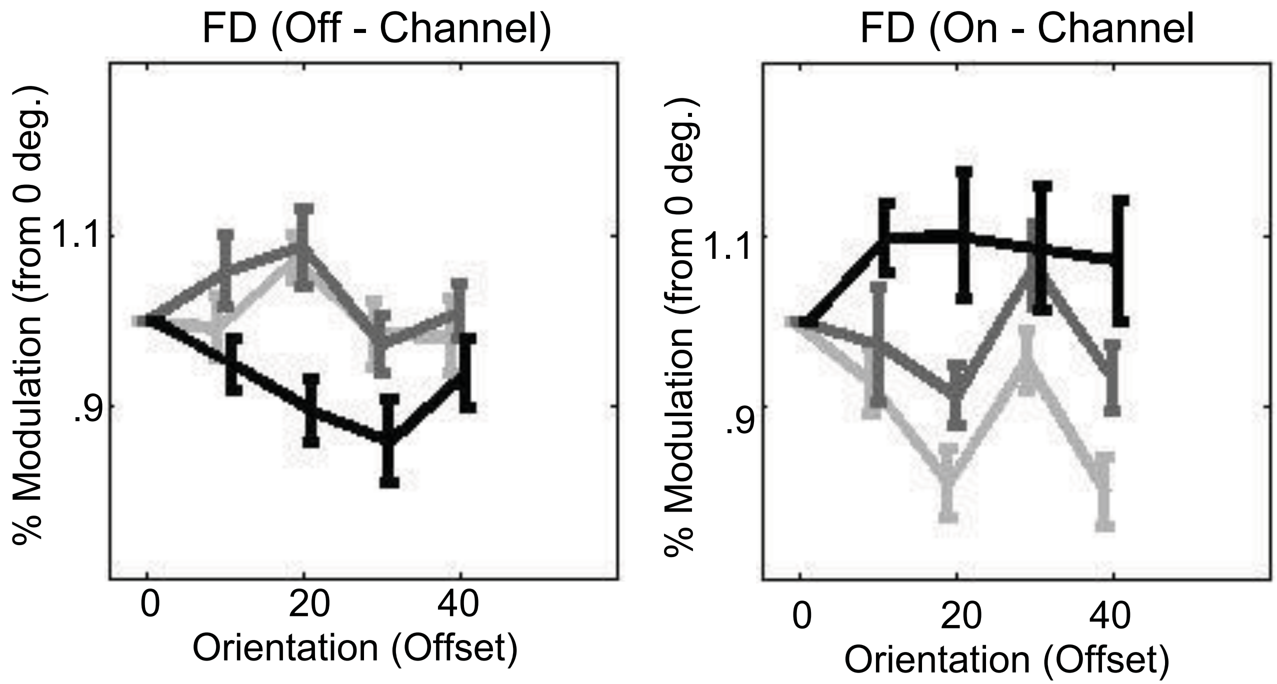
FD (Off - Channel)
% Modulation (from 0 deg.)
1.1
.9
0
20
40
Orientation (Offset)
FD (On - Channel
% Modulation (from 0 deg.)
1.1
.9
0
20
40
Orientation (Offset)